

Improving the Yield and Rate of Acid-Catalyzed Deconstruction of Lignin by Mechanochemical Activation

Darpan H. Patel,^[a] Dominik Marx,^[b] and Allan. L. L. East*^[a]

Lignin is a potential biomass feedstock from plant material, but it is particularly difficult to economically process. Inspired by recent ball-milling results, state-of-the-art quantum mechanochemistry calculations have been performed to isolate and probe the purely mechanochemical stretching effect alone upon acid-catalyzed deconstruction of lignin. Effects upon cleavage of several exemplary simple ethers are examined first, and with low stretching force they all are predicted to cleave substantially faster, allowing for use of milder acids and lower temperatures. Effects upon an experimentally known lignin fragment model (containing the ubiquitous β -O-4 linkage) are next examined; this first required a mechanism refinement (3-

step indirect cleavage, 1-step side reaction) and identification of the rate-limiting step under zero-force (thermal) conditions. Mechanochemical activation using very low stretching forces improves at first only yield, by fully shutting off the ring-closure side reaction. At only somewhat larger forces, in stark contrast, a switch in mechanism is found to occur, from 3-step indirect cleavage to the direct cleavage mechanism of simple ethers, finally strongly enhancing the cleavage rate of lignin. It is concluded that mechanochemical activation of the common β -O-4 link in lignin would improve the rate of its acidolysis via a mechanism switch past a low force threshold. Relevance to ball-milling experiments is discussed.

1. Introduction

Lignin is a carbohydrate biopolymer, containing phenylpropane monomer units cross-linked by ether linkages, which provides microbial resistance and structural rigidity to plants.^[1] In biomass applications, a broad range of valuable bulk chemicals and biofuels, particularly aromatic compounds, are potentially derivable from lignin, and hence a variety of well-established techniques have been researched, using chemical, thermal, enzymatic and microbial approaches.^[1–5] One such research strategy, nicknamed “lignin-first,” involves extraction and processing of lignin concurrently,^[6] while another approach, dubbed “bottom-up,” focuses on the mechanism of the transformation of lignin fragments and then applies the methods in the lignin conversion.^[7] However, lignin is notoriously recalcitrant towards processing, to date requiring harsh conditions and environmentally unfriendly agents (e.g. strong acids), and research continues for other means of deconstructing lignin.

Mechanochemistry, the chemistry of mechanically activated molecules, offers a different means of activating molecules for reaction by imparting energy in particular ways that scale up to industrial applications.^[8] Three major techniques employed in industrial mechanochemistry are ball-milling,^[9,10] sonochemistry,^[11] and tribochemistry.^[12] Pioneering work has

demonstrated the application of mechanochemical activation of cellulose to obtain oligosaccharides,^[13] sugar alcohols,^[14] and furfurals^[15] with high yield^[16–18] in astonishingly mild conditions. The underlying reasons for the enormous mechanochemical rate accelerations seen for cellulose,^[19] as well as a protein mimic in recent force-clamp-mode atomic force microscopy (AFM) experiments,^[20] have been probed recently to generate further insight in the burgeoning field of biomass mechanochemistry.

Interestingly, experimental research on mechanochemical means of processing lignin has a rich history. It appears to have begun with the pre-1960 discovery of inadvertent mechanochemistry in the mechanical processing of wood in the pulp and paper industry.^[21] In 1970–71, Siminescu et al. reported “destruction” of lignin during milling in a nitric oxide atmosphere, suspecting homolytic scission generating radicals.^[22] Subsequently, Sumimoto et al. studied ball-milling of pulp^[23] and small molecular models of lignin.^[24–27] They, and Choudhury et al.,^[28] linked photodegradation (so-called “yellowing”) of wood pulp to the inadvertent creation of small chromophoric molecules during mechanical pulping. More recent ball-milling studies of lignin or lignin fragments have tended to involve ball-milling strategies using solid reagents (hydroxide,^[29–31] oxidant,^[32] or others^[33]) to deliberately crack^[29,30,32] or modify^[31,33] lignin for valorization. While Rinaldi and Schüth and co-workers have shown that the combination of acid catalysis with concurrent ball-milling can generate water-soluble lignin fragments from wood^[13] (up to roughly 4000 Daltons or 25-monomer segments^[18]), mechanistic details about how this small fraction of total intermonomer bonds was broken, or whether this fraction can be improved (e.g. tribochemistry^[12]), are unknown.

Hence, in this work we systematically explore the exclusive effect of external stretching force on acid-catalyzed lignin

[a] D. H. Patel, Prof. Dr. A. L. L. East
Department of Chemistry and Biochemistry
University of Regina
Regina SK S4S 0A2 (Canada)
E-mail: allan.east@uregina.ca

[b] Prof. Dr. D. Marx
Lehrstuhl für Theoretische Chemie
Ruhr-Universität Bochum
44780 Bochum (Germany)

Supporting information for this article is available on the WWW under <https://doi.org/10.1002/cphc.202000671>

cleavage, using computational modelling. Although our motivation clearly comes from large-scale applications mainly using ball milling technologies, we and others cannot realistically model all the intricate processes that contribute to mechanochemical reactions in ball mills down to the level of the quantum chemical elementary cleavage reactions that require accurate electronic structure methods. Moreover, it is well-known that local heating effects as well as non-negligible molecular interactions with the balls might contribute on top of genuine mechanical activation to the success of ball milling, also in the realm of biomass deconstruction. Thus, our general strategy is to isolate the purely-mechanochemical stretching effect, by taking recourse to the well-validated approaches of computational mechanochemistry, where collinear tensile forces are applied to mechanically stretch the computationally tractable fragment of the macromolecule of interest.^[8] This approach allows for quantum mechanochemical analyses of force-activated chemical reactions, much as standard quantum chemistry has contributed significantly for decades to understand the mechanisms of thermally or photochemically activated chemical reactions. Let us mention in passing that our state-of-the-art modelling used here, the so-called isotensional (or EFEI) approach to computational mechanochemistry^[8] paired with semicontinuum solvation modelling,^[34–36] (see Supporting Information Section 1 for background and details), recently successfully reproduced (and thus elucidated) the surprising mechanochemical bond cleavage results in the aforementioned force-clamp-mode AFM experiments on mechanochemical peptide bond cleavage.^[20] Although our approach obviously does not microscopically mimic ball-milling setups, the effect it isolates can be probed and thus quantified experimentally in such single-molecule force probe measurements.^[8]

Recognizing that the key bond to break in lignin is an ether bond, we first present results for several simple ethers as benchmark modelling.^[37] As expected, we found significant improvement, as well as some “disfavoring” force regimes for some (but not all) ether cases. Then in the core part of this work, we performed a comprehensive computational stretching-mechanochemistry study of the acid-catalyzed cleavage of a model lignin. This model fragment is based on detailed previous thermal (i.e. not mechanochemical) work of Sturgeon et al.^[38] who introduced and tested four models experimentally and offered density-functional (DFT) computations of potential intermediates. Sturgeon et al. performed experimentally the acid-catalyzed cleavage of four lignin model compounds having the common “β-O-4” ether linkage (a linkage still commonly remaining in the Rinaldi and Schüth ball-milling experiments^[16]), at 150 °C using 0.2 M H₂SO₄. Product yield was limited to ~75% due to charring at these harsh conditions, but the ether cleavage yield was especially poor (36–39%) for their so-called HH fragment (as depicted in Figure 1) due to an additional side reaction, a ring closure, in 37% yield. Hence for our mechanochemistry study we chose their more interesting and low-yield HH example. Since the thermal mechanism of cleavage is significantly more complex than that of simple ethers, we first had to determine rate-limiting transition states and activation energies for the proposed mechanisms of Sturgeon et al. via

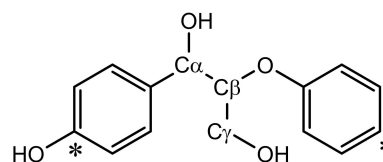


Figure 1. Lignin model compound HH (H = p-hydroxyphenyl) Asterisks denote the *para* carbons pulled in opposing directions in the quantum mechanochemistry calculations.

standard zero-force computations before we could perform mechanochemistry calculations on them. Once we finished the HH-lignin mechanochemistry calculations, we found, instead of simple rate acceleration, a potentially key surprise: as a function of increasing mechanochemical activation, first (at low forces) a predicted initial improvement in *yield only* by disfavoring the ring-closure side reaction, followed (at higher forces) by a *switch in mechanism* that additionally predicts significant rate acceleration. Overall, simple mechanochemical activation is predicted to enhance first the yield and then the rate of lignin deconstruction.

2. Results and Discussion

2.1. Mechanochemical Cleavage of Simple Ethers

We first examined the single-step acid-catalyzed “direct” cleavage of the ether linkage (Figure 2) for six different simple ethers, in five cases varying only the X substituents (H or Me), and in the sixth case replacing the C_eC_f ethyl group with an aromatic ring as in lignin. Note the important dihedral angle $\alpha = \alpha(C_e C_b C_a O_d)$ in the figure. It prefers to be clinal ($\alpha \approx 90^\circ$) at the transition state (when the external stretching force $F = 0$ nN), but upon reverse descent towards reactants (from the transition state on the potential energy surface) the reaction path bifurcates to *trans* ($\alpha \approx 180^\circ$) and *gauche* ($\alpha \approx 60^\circ$) reactant conformer possibilities. For activation energy computation the *trans* conformer was assumed for the reactant ether, because it would quickly dominate any equilibrium distribution when $F > 0$ nN.

Figure 2 shows the computed activation free energies as a function of stretching force applied. Most importantly, at $F > 0.8$ nN, activation free energies are predicted to have fallen dramatically (1 kcal mol⁻¹ per added 0.1 nN) for all six cases. Additionally, what is quite interesting are the substitution effects revealed in Figure 2. For small forces of ≈ 0.1 nN, a barrier rise (an inhibition, or rate retardation) is seen in the four cases having no C_b substitution, identical to what has been seen before^[37] for the similar but anionic S_N2 system of ether + ethoxide. This retardation is due to making the $\alpha \approx 90^\circ$ dihedral angle of the transition state (the “clinal pocket”) more difficult to achieve. Contrastingly, the two neo cases with their C_b methyl substituents have no “clinal pocket” at $F = 0$ nN and thereby immediately benefit from external force. At larger forces, eventually the continued weakening of the ether C–O

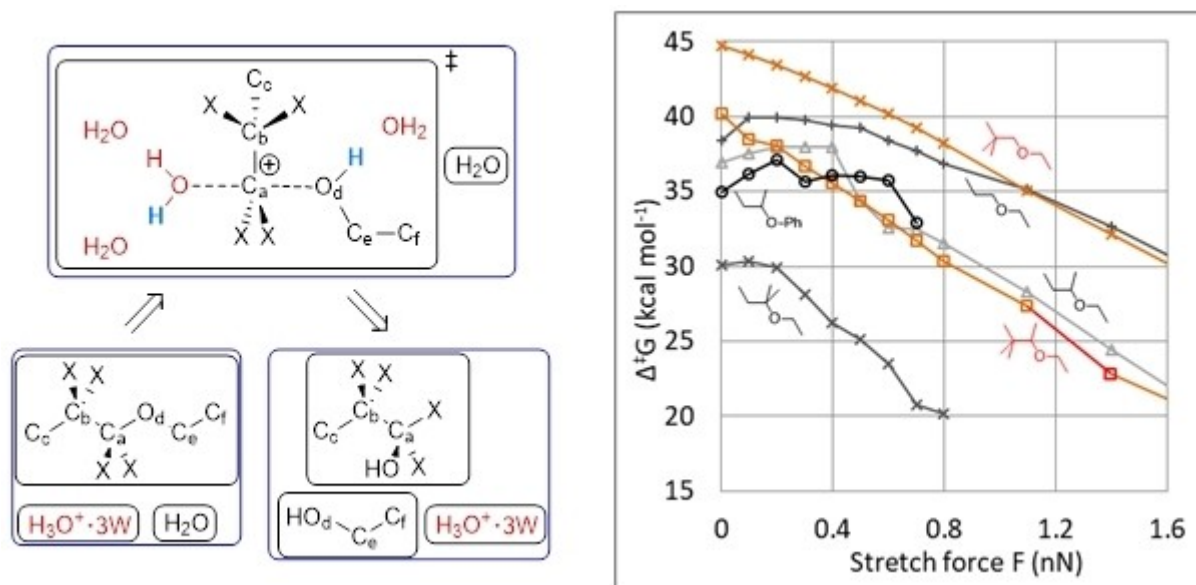


Figure 2. Computed activation free energies vs. stretching force applied, for acid-catalyzed cleavage of simple ethers. The direct one-step mechanism, displayed at left, indicates the transferring H^+ atoms in blue in the transition state (arising from H_3O^+ ions in the reactant and product states). Each circled entity is a separate calculation. The plot at right reveals activation energy magnitudes determined by substitution at the $\text{S}_{\text{N}}2$ carbon C_a : e.g. barriers of {37, 38, 31, 20} kcal mol^{-1} for {primary, secondary, tertiary} ethers at $F=0.8$ nN. At small forces, initial barrier rises are seen in the four cases where no substitution exists on the adjacent carbon (C_b in Figure 2). Steps occur in the curves at forces at which internal rotation barriers have been overcome, e.g. clinal \rightarrow trans ($\alpha(\text{C}_5\text{C}_6\text{O}_d)$) changes at 0.4–0.7 nN, and a phenyl rotation at 0.25 nN.

bond causes the activation free energy values to fall in all cases, at a substantial and relatively common rate (~ 1 kcal mol^{-1} per 0.1 nN added), and the barriers eventually show only C_a substitution effects, e.g. barriers of {37–38, 31, 20} kcal mol^{-1} for {primary, secondary, tertiary} ethers at $F=0.8$ nN.

To conclude this section, (i) mechanochemical activation is predicted to greatly assist acid-catalyzed “direct” ether cleavage, allowing for use of significantly lower temperatures for cleavage, and (ii) it is predicted to be especially beneficial for the sterically protected neo cases (maximal branching at the carbon adjacent to the $\text{S}_{\text{N}}2$ carbon). The significant reductions in activation energy here motivated us to pursue the more complex case of ether cleavage in lignin deconstruction.

2.2. Refined Mechanism for Thermal Acid-Catalyzed Lignin Cleavage

More complex ethers can have more complex mechanisms for cleavage, and lignin is a good example of this. The complexity arises due to the α - and γ -hydroxyl groups near the β -ether linkage (Figure 1). The first hydrated proton preferentially attacks the α -hydroxyl oxygen, not the β -ether linkage, resulting in a dehydration step which complicates the mechanism. Sturgeon et al.^[38] proposed multistep intermediate pathways (Supplementary Information) for the observed “indirect” cleavage (route I) and ring-closing (route II) pathways, based on their observed product distributions and their exploratory DFT optimizations. Building upon these pathways, we performed transition state determinations, needed to identify the rate-

limiting steps of each pathway, as well as for ensuing barrier height computation for these rate-limiting steps at various values of added mechanochemical force. We employed Eigen-ion-based semicontinuum modelling (Figure S2) for improved accuracy, but kept their level of DFT (M06-2X/6-311++G(d,p)/CPCM//M06-2X/6-31G(d)/CPCM). Their proposed cationic intermediates were generally *not* stationary points (i.e. true intermediates) once the explicit water molecules were in place, computationally supporting with our solvation approach the proposal by Cox^[39] that such cations generally not be listed as intermediates in aqueous chemistry. This reduces the number of relevant transition states for the mechanisms.

The refined thermally activated mechanisms determined by us including local solvation appear in Figure 3. Route I, the observed low-yield “indirect” ether cleavage, is now a three-step mechanism, each step being acid-catalyzed: dehydration to HH-3, rehydration to HH-6, and a non-hydrolytic ether cleavage. Route II, the observed ring closure of HH, is now better represented as a single asynchronous concerted step, containing dehydration followed by immediate ring closure and then immediate C–H proton loss, with the transition state (TS9) occurring during the ring closure moment. Route III, the single-step direct ether cleavage mechanism (Figure 2), is included in Figure 3 for completeness, for although this was not observed in the thermal-limit (i.e. zero external force) Sturgeon et al. experiments on HH,^[38] it might become relevant once mechanochemical force is applied. The structures of the five relevant transition states, including the location of explicit solvation waters employed in the modeling, appear in Figure S2.

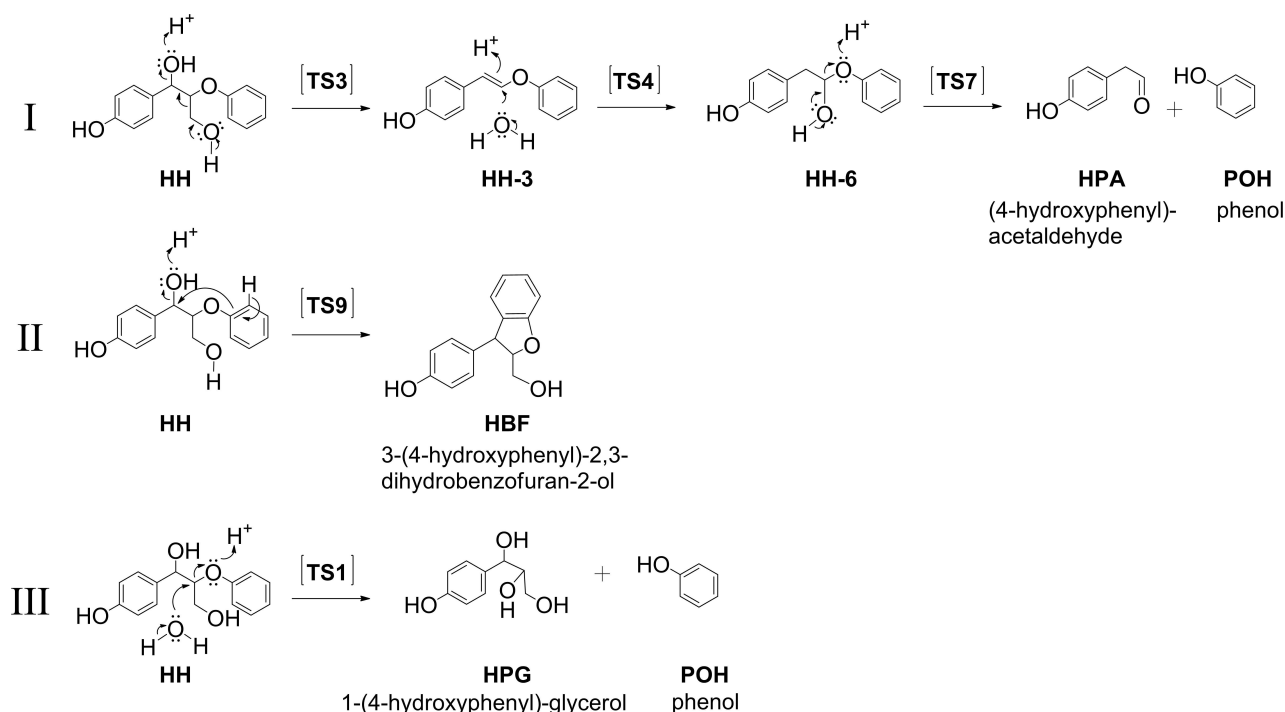


Figure 3. Mechanisms for the three processes considered for acid-catalyzed mechanochemistry of HH. Routes I and II are refined (see the Supporting Information) mechanisms for the observed^[38] products from thermal-limit (non-mechanochemically assisted) experiments, while Route III is for a potential mechanochemically activated pathway not observed in the thermal-limit experiments.

The associated Gibbs free energies from zero-force computations (Figure 4) show that this proper treatment of H_3O^+ as an explicitly solvated Eigen cation ($\text{H}_3\text{O}^+ \cdot 3 \text{W}$) provides results that agree (within a tolerable 3 kcal mol^{-1} error) with the 50:50 product distribution that has been experimentally found by Sturgeon et al.^[38] in the thermal reaction: both product channels are seen to have very similar overall activation energies (namely 29 and 32 kcal mol^{-1} for $\text{HH} \rightarrow \text{TS4}$ and $\text{HH} \rightarrow \text{TS9}$, respectively). Importantly, the rate-limiting transition state in the three-step

indirect cleavage pathway is TS4, the transition state of the *rehydration middle step* (not the cleavage step!), which is very important, since we will see (next section) that this renders this route somewhat insensitive to mechanochemical improvement of its rate. This successful application of semicontinuum modeling has provided an improved mechanistic representation (and the rate-limiting steps) for the two experimentally observed thermal product channels, which now allows us to probe mechanochemical effects in the next section.

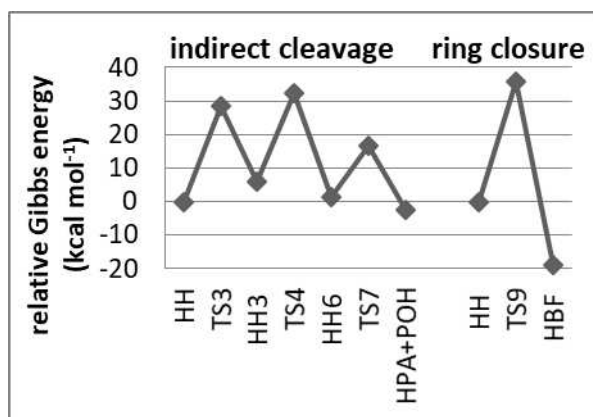


Figure 4. Reaction Gibbs free energy profiles for the two experimentally observed product channels for thermally activated acid-catalyzed lignin deconstruction using the lignin fragment model HH: The three-step dehydration/rehydration/cleavage I (left) and the single-step ring closure II (right). See Figure 3 for mechanism and Figure S2 for modelling.

2.3. Mechanochemical Cleavage of Lignin

At this stage, computational mechanochemistry was performed on the reactant HH structure and the three potentially rate-limiting transition states for the three pathways in Figure 3 (TS1, TS4, TS9). These energies are used for computation of overall activation Gibbs free energies for each product channel (i.e. $\text{HH} \rightarrow \text{TS1}$, $\text{HH} \rightarrow \text{TS4}$, and $\text{HH} \rightarrow \text{TS9}$) in the presence of a constant external force that is systematically increased. The stretching force was applied to the two para carbons of the two end aromatic rings (see Figure 1), using values of F ranging from 0.2 to 4.2 nN.

The resulting activation Gibbs energies are plotted in Figure 5 and exhibit a stunning menagerie of effects made possible by mechanochemical activation. Qualitatively, the effects are rather simply linked to the degree of alignment of the dominant motion vector at the transition state in the

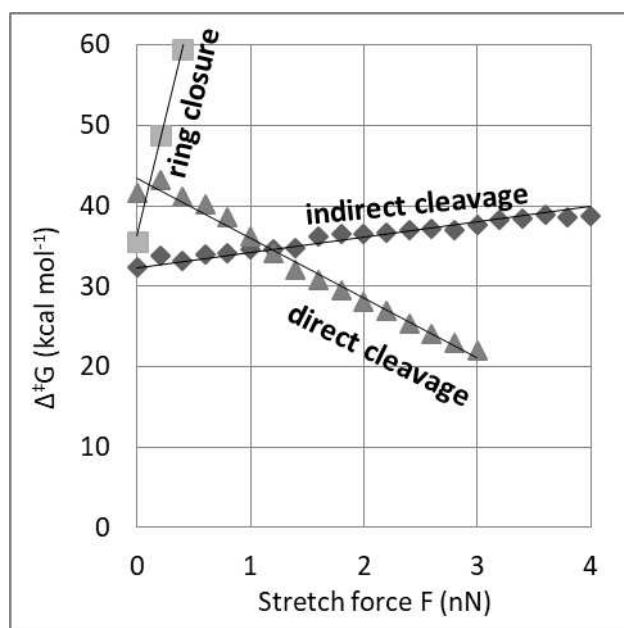


Figure 5. Computed activation Gibbs free energies of lignin model HH versus stretching force applied.

forward direction to the external force vector R_{AB} , as we now explain.

For Route I (indirect cleavage), the rate-limiting transition state is TS4, a rehydration stage in which the transition mode features mainly proton transfer from adjacent hydronium to the C=C unit of HH3 intermediate. As this transfer direction is largely perpendicular to the R_{AB} stretch direction (see step Ib in Figure S2), this barrier is rather insensitive to the external stretch force. (Only a mild increase in barrier is predicted by the calculations).

For Route II (ring closure), its only significant transition state is TS9. Its transition mode features mainly approach of two C atoms (C–C bond formation), an approach that is antiparallel to the R_{AB} stretch direction (see step II in Figure S2). Thus, this motion is greatly disfavored by external R_{AB} stretching, and its barrier rises dramatically.

For Route III (direct cleavage), its only significant transition state is TS1. Its transition mode, at the transition state, is an S_N2 substitution mode, involving primarily a move of a carbon atom away from its bonded ether oxygen and towards a water oxygen. Since half of this mode is of a direction somewhat parallel to the R_{AB} stretch direction, this motion is favored by external R_{AB} stretching, and its barrier falls significantly, as we observed with the simple ethers (Figure 2).

These three transition states thus exhibit three completely different responses to external stretching force. What will be observed experimentally will depend on which channel has the lowest activation Gibbs free energy at a particular stretch force. At zero force, the Sturgeon et al. experiment shows a 50:50 product distribution,^[38] because TS4 and TS9 are close in energy, and TS1 is too high to be competitive. Figure 5 shows the predicted effects of force. Initially, for forces up to 1.2 nN,

the predicted effect would be an improved yield of ether cleavage, because TS9 (for ring closure) immediately rises in energy and loses its competitiveness. However, the rate is not improved (and mildly harmed), for TS4 (for indirect cleavage) is rather insensitive to force. Later, at the rather mild force of $F = 1.2$ nN, the rate of ether cleavage is predicted to suddenly dramatically improve, due to a *switch in mechanism*: the direct cleavage barrier over TS1, which at $F = 0$ nN is not competitive (41 kcal mol⁻¹), has been lowered to the point where it crosses below the indirect-cleavage rate-limiting barrier. Past this point, at larger forces, the direct cleavage scenario is predicted to become the dominant reaction route, and the cleavage rate finally shows a dramatic enhancement due to significantly lowering furthermore the reaction barrier due to mechanochemical activation. Additionally, the barrier should come low enough that less harsh acid conditions could be used, reducing the amount of charring which would improve yield even further. Figure 6 summarizes these different scenarios which greatly depend on the force regime.

3. Conclusions

The impact of mechanochemical activation upon aqueous acid-catalyzed deconstruction of a lignin fragment was isolated, using quantum mechanochemical methods that take local solvation effects explicitly into account. Key results are (i) outstanding benefits for lignin depolymerization in both cleavage yield and rate are predicted, and (ii) the mechanistic explanations for all qualitative features (including the presence of a force threshold needed for rate improvement) are provided.

In order to set the stage for tackling the complex lignin deconstruction process by cleaving its ether linkage, our computations on six simple ethers showed that all of them are subject to a direct bond cleavage process and eventually feature pronounced reaction barrier reductions from mechanochemical stretching. This allows for more benign reaction conditions for their acid-catalyzed mechanochemical cleavage with reference to pure thermal activation. Qualitative substituent effects were also observed: only substitutions at C_a (the S_N2 carbon) are important at high forces, but at purely thermal (zero-external-force) conditions a “clinal pocket” effect is seen to “create” lowered barriers if the molecule is devoid of C_b substitutions.

Lignin is a significantly more complex ether that features a much more complex cleavage mechanism. Based on existing literature, we first of all determined the multistep mechanism for the previously experimentally observed^[38] thermally activated acid-catalyzed “indirect” cleavage of a lignin fragment, where explicit solvation by water molecules turned out to be key to obtain agreement with experimental data for its low yield (vs. an observed and undesired ring-closure side reaction). The indirect cleavage route, which arises because the acid first protonates a hydroxyl group near the ether moiety rather than the ether moiety itself, was here found to be a three-step sequence critically involving dehydration, rehydration, and α -

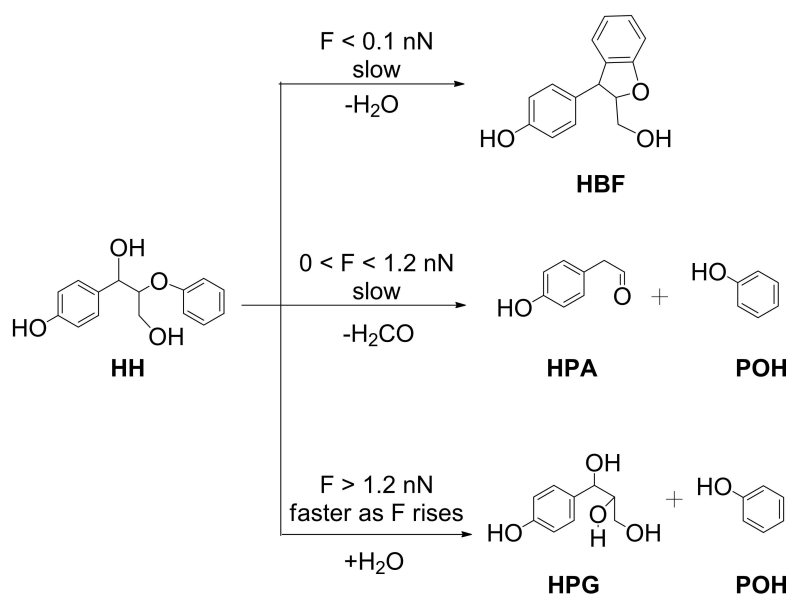


Figure 6. Summary of the disclosed reaction pathways and products under various magnitudes of mechanochemical stretching force applied, according to the computational mechanochemistry predictions (Figure 5). The hydroxyphenyl glycol (HPG) product may feature additional acid-catalyzed dehydration, depending on experimental factors.

hydroxyether cleavage. Importantly, it is the rehydration step that is rate limiting and not bond cleavage of the ether linkage itself. This complexity in the cleavage mechanism of lignin versus simple ethers completely changes the effect of mechanochemical stretching upon ether bond cleavage, for without a dissociative component to the rate-limiting transition state, the external stretching should be unable to improve the cleavage rate.

After this initial surprise of an unexpected rate-limiting step in case of lignin, two more surprises were discovered during the ensuing mechanochemistry calculations. First, though the indirect-cleavage rate-limiting barrier was seen to actually increase with force, the yield of this channel immediately improved, due to the dramatically raised activation energy for the ring-closure side reaction. Thus, even low forces effectively suppress the generation of that unwanted side product of lignin depolymerization. Second, at a force of only 1.2 nN, a switch in mechanism is found, with the direct-cleavage pathway (i) suddenly offering the by far lowest-energy channel to cleavage, and (ii) an activation barrier that steeply decreases as a function of force, finally dramatically improving also the cleavage rate of lignin. Based on these findings, we conclude that mechanochemical activation of acid-catalyzed lignin depolymerization in aqueous media leads to systematic improvements of yield and rate, which could eventually become highly beneficial for deconstructing such naturally occurring biopolymers into valuable chemicals.

A logical next step, from the presented computational prediction (using a rather small molecular lignin fragment) that a force threshold for rate improvement exists, is an utmost controlled experiment, such as force-clamp AFM where the magnitude of the force applied at the single-molecule level can be precisely controlled. This step would require the chemical

embedding of suitable lignin fragments into macromolecular linker chains, which in turn must be chemically anchored to the AFM tip and a reference surface, subject to all required cross-check as to excluding alternative mechanochemical cleavage channels which might interfere with lignin deconstruction. Such an experimental endeavor seems justified, given the scenario that has been predicted here using a proven quantum mechanochemistry technique that successfully reproduced force-threshold phenomena in similar experiments performed for amide hydrolysis (see Introduction). Should this be successful, a return to ball-mill or other mechanochemistry-based investigations for acid-assisted lignin deconstruction may be encouraged.

Acknowledgements

ALLE acknowledges support from his NSERC Discovery Grants 238871-2012, RGPIN-2017-06247) and his CFI Leading Edge Fund2009 grant 21625. DM acknowledges partial support from his DFG Koselleck Grant (MA1547/9). Funded by Deutsche Forschungsgemeinschaft (DFG, German Research Foundation) under Germany's Excellence Strategy-EXC 2033-390677874-RESOLV. We are particularly grateful for the RESOLV Visiting Professorship of ALLE at the Center for Solvation Science ZEMOS at Ruhr-Universität Bochum.

Conflict of Interest

The authors declare no conflict of interest.

Keywords: biomass · ether cleavage · lignin acidolysis · mechanochemistry

- [1] J. Zakzeski, P. C. A. Bruijninx, A. L. Jongerius, B. M. Weckhuysen, *Chem. Rev.* **2010**, *110*, 3552–3599.
- [2] T. D. H. Bugg, M. Ahmad, E. M. Hardiman, R. Singh, *Curr. Opin. Biotechnol.* **2011**, *22*, 394–400.
- [3] S. P. S. Chundawat, G. T. Beckham, M. E. Himmel, B. E. Dale, *Annu. Rev. Chem. Biomol. Eng.* **2011**, *2*, 121–145.
- [4] A. J. Ragauskas, G. T. Beckham, M. J. Bidy, R. Chandra, F. Chen, M. F. Davis, B. H. Davison, R. A. Dixon, P. Gilna, M. Keller, P. Langan, A. K. Naskar, J. N. Saddler, T. J. Tschaplinski, G. A. Tuskan, C. E. Wyman, *Science* **2014**, *344*, 1246843.
- [5] R. Rinaldi, R. Jastrzebski, M. T. Clough, J. Ralph, M. Kennema, P. C. A. Bruijninx, B. M. Weckhuysen, *Angew. Chem. Int. Ed.* **2016**, *55*, 8164–8215; *Angew. Chem.* **2016**, *128*, 8296–8354.
- [6] a) S. De, J. Zhang, R. Luque, N. Yan, *Energy Environ. Sci.* **2016**, *9*, 3314–3347; b) P. Ferrini, C. A. Rezende, R. Rinaldi, *ChemSusChem* **2016**, *9*, 3171–3180; c) P. Ferrini, R. Rinaldi, *Angew. Chem. Int. Ed.* **2014**, *53*, 8634–8639; *Angew. Chem.* **2014**, *126*, 8778–8783; d) M. V. Galkin, J. S. M. Samec, *ChemSusChem* **2014**, *7*, 2154–2158; e) T. Renders, S. Van den Bosch, T. Vangeel, T. Ennaert, S. F. Koelewijn, G. Van den Boscche, C. M. Courtin, W. Schutyser, B. F. Sels, *ACS Sustainable Chem. Eng.* **2016**, *4*, 6894–6904.
- [7] C. Zhang, H. Li, J. Lu, X. Zhang, K. E. MacArthur, M. Heggen, F. Wang, *ACS Catal.* **2017**, *7*, 3419–3429.
- [8] a) M. K. Beyer, H. Clausen-Schaumann, *Chem. Rev.* **2005**, *105*, 2921–2948; b) M. M. Caruso, D. A. Davis, Q. Shen, S. A. Odom, N. R. Sottos, S. R. White, J. S. Moore, *Chem. Rev.* **2009**, *109*, 5755–5798; c) J. Ribas-Arino, D. Marx, *Chem. Rev.* **2012**, *112*, 5412–5487; d) T. Stauch, A. Dreuw, *Chem. Rev.* **2016**, *116*, 14137–14180.
- [9] a) J. G. Hernández, C. Bolm, *J. Org. Chem.* **2017**, *82*, 4007–4019; b) J.-L. Do, T. Friščić, *Synlett* **2017**, *28*, 2066–2092; c) J.-L. Do, T. Friščić, *ACS Cent. Sci.* **2017**, *3*, 13–19.
- [10] a) J. Andersen, J. Mack, *Green Chem.* **2018**, *20*, 1435–1443; b) J. L. Howard, Q. Cao, D. L. Browne, *Chem. Sci.* **2018**, *9*, 3080–3094; c) C. Bolm, J. G. Hernández, *ChemSusChem* **2018**, *11*, 1410–1420; d) D. Tan, T. Friščić, *Eur. J. Org. Chem.* **2018**, 18–33.
- [11] a) K. S. Suslick, *Faraday Discuss.* **2014**, *170*, 411–422; b) N. Kardos, J.-L. Luche, *Carbohydr. Res.* **2001**, *332*, 115–131; c) J. Lindley, T. J. Mason, *Chem. Soc. Rev.* **1987**, *16*, 275–311.
- [12] T. E. Fischer, *Ann. Rev. Mater. Sci.* **1988**, *18*, 303–323.
- [13] N. Meine, R. Rinaldi, F. Schüth, *ChemSusChem* **2012**, *5*, 1449–1454.
- [14] J. Hilgert, N. Meine, R. Rinaldi, F. Schüth, *Energy Environ.* **2013**, *6*, 92–96.
- [15] R. Carrasquillo-Flores, M. Kåldström, F. Schüth, J. A. Dumesic, R. Rinaldi, *ACS Catal.* **2013**, *3*, 993–997.
- [16] M. Kåldström, N. Meine, C. Fares, R. Rinaldi, F. Schüth, *Green Chem.* **2014**, *16*, 2454–2462.
- [17] R. M. Kaufman Rechulski, D. Marcelo, M. Kåldström, U. Richter, F. Schüth, R. Rinaldi, *Ind. Eng. Chem. Res.* **2015**, *54*, 4581–4592.
- [18] G. Calvaruso, M. T. Clough, R. Rinaldi, *Green Chem.* **2017**, *19*, 2803–2811.
- [19] S. Amirjalayer, H. Fuchs, D. Marx, *Angew. Chem. Int. Ed.* **2019**, *58*, 5232–5235.
- [20] M. F. Pill, A. L. L. East, D. Marx, M. K. Beyer, H. Clausen-Schaumann, *Angew. Chem. Int. Ed.* **2019**, *58*, 9787–9790.
- [21] J. C. Pew, *Tappi J.* **1957**, *40*, 553–558.
- [22] a) Simionescu, C. Grigoras, M. Mechano, *Cellulose. Chem. Technol.* **1970**, *4*, 421–432; b) Grigoras M. Bulacovschi, V. Rozmarin, G. Simionescu, *Cellulose Chem. Technol.* **1971**, *5*, 471–487.
- [23] a) H. Hirashima, M. Sumimoto, *Mokuzai Gakkaishi* **1986**, *32*, 705–712; b) M. Sumimoto, *Mokuzai Gakkaishi* **1990**, *36*, 783–796.
- [24] D. Y. Lee, S. Tachibana, M. Sumimoto, *Cellulose Chem. Technol.* **1988**, *22*, 201–210.
- [25] a) D. Y. Lee, M. Sumimoto, *Holzforchung* **1990**, *44*, 347–350; b) D. Y. Lee, M. Matsuoka, M. Sumimoto, *Holzforchung* **1990**, *44*, 415–418; c) D. Y. Lee, M. Sumimoto, *Holzforchung* **1991**, *45*, 15–20; d) Z.-H. Wu, M. Sumimoto, H. Tanaka, *Holzforchung* **1994**, *48*, 395–399; e) Z. H. Wu, M. Sumimoto, H. Tanaka, *Holzforchung* **1994**, *48*, 400–404.
- [26] a) Z.-H. Wu, M. Matsuoka, D. Y. Lee, M. Sumimoto, *Mokuzai Gakkaishi* **1991**, *37*, 164–171; b) Z.-H. Wu, M. Sumimoto, *Mokuzai Gakkaishi* **1992**, *38*, 277–284; c) K. Itoh, S. Tachibana, M. Sumimoto, *Sen'i Gakkaishi* **1992**, *48*, 112–119; d) K. Itoh, S. Tachibana, M. Sumimoto, H. Tanaka, *Sen'i Gakkaishi* **1992**, *48*, 625–634; e) K. Itoh, M. Sumimoto, S. Tachibana, *Sen'i Gakkaishi* **1993**, *49*, 569–575.
- [27] a) Z.-H. Wu, M. Sumimoto, H. Tanaka, *J. Wood Chem. Technol.* **1995**, *15*, 27–42; b) Z.-H. Wu, M. Sumimoto, H. Tanaka, *ACH - Models Chem.* **1994**, *131*, 571–580; c) K. Itoh, M. Sumimoto, H. Tanaka, *J. Wood Chem. Technol.* **1995**, *15*, 395–411; d) Z.-H. Wu, K. Katayama, M. Sumimoto, H. Tanaka, *J. Fac. Agric. Kyushu Univ.* **1995**, *40*, 19–27.
- [28] H. Choudhury, S. Collins, R. S. Davidson, A. Castellan, *Current Trends in Polymer Photochemistry* **1995**, 211–218.
- [29] T. Kleine, J. Buendia, C. Bolm, *Green Chem.* **2013**, *15*, 160–166.
- [30] A. D. Brittain, N. J. Chrisandina, R. E. Cooper, M. Buchanan, J. R. Cort, M. V. Olarte, C. Sievers, *Catal. Today* **2018**, *302*, 180–189.
- [31] S. G. Yao, J. K. Mobley, J. Ralph, M. Crocker, S. Parkin, J. P. Selegue, M. S. Meier, *ACS Sustainable Chem. Eng.* **2018**, *6*, 5990–5998.
- [32] S. Dabral, H. Wotruba, J. G. Hernández, C. Bolm, *ACS Sustainable Chem. Eng.* **2018**, *6*, 3242–3254.
- [33] a) M. J. Rak, T. Friščić, A. Moores, *Faraday Discuss.* **2014**, *170*, 155–167; b) M. J. Rak, T. Friščić, A. Moores, *RSC Adv.* **2016**, *6*, 58365–58370; c) X. Guo, X. Junna, M. P. Wolcott, J. Zhang, *ChemistrySelect* **2016**, *1*, 3449–3454; d) C. Schneidermann, N. Jaeckel, S. Oswald, L. Giebeler, V. Presser, L. Borchardt, *ChemSusChem* **2017**, *10*, 2416–2424; e) U. Weissbach, S. Dabral, L. Konnert, C. Bolm, J. G. Hernández, *Beilstein J. Org. Chem.* **2017**, *13*, 1788–1795.
- [34] a) S. W. Rick, B. J. Berne, *J. Am. Chem. Soc.* **1994**, *116*, 3949–3954; b) J. R. Pliego Jr., J. M. Riveros, *J. Phys. Chem. A* **2001**, *105*, 7241–7247; c) C. P. Kelly, C. J. Cramer, D. G. Truhlar, *J. Phys. Chem. A* **2006**, *110*, 2493–2499; d) F. Khalili, A. Henni, A. L. L. East, *J. Mol. Struct. THEOCHEM* **2009**, *916*, 1–9; e) K. Z. Sumon, A. Henni, A. L. L. East, *Ind. Eng. Chem. Res.* **2012**, *51*, 11924–11930; f) K. Z. Sumon, C. H. Bains, D. J. Markewich, A. Henni, A. L. L. East, *J. Phys. Chem. B* **2015**, *119*, 12256–12264.
- [35] S. Dhillon, A. L. L. East, *Int. J. Quantum Chem.* **2018**, *118*, e25703.
- [36] V. S. Bryantsev, M. S. Diallo, W. A. Goddard III, *J. Phys. Chem. B* **2008**, *112*, 9709–9719.
- [37] M. Krupička, D. Marx, *J. Chem. Theory Comput.* **2015**, *11*, 841–846.
- [38] M. R. Sturgeon, S. Kim, K. Lawrence, R. S. Paton, S. C. Chmely, M. Nimlos, T. D. Foust, G. T. Beckham, *ACS Sustainable Chem. Eng.* **2014**, *2*, 472–485.
- [39] R. A. Cox, *Can. J. Chem.* **2012**, *90*, 811–818.

Manuscript received: July 31, 2020

Accepted manuscript online: August 26, 2020

Version of record online: November 23, 2020